

1 **Simultaneous factor analysis of organic particle and gas**  
2 **mass spectra: AMS and PTR-MS measurements at an**  
3 **urban site**

4

5 **J. G. Slowik<sup>1,3</sup>, A. Vlasenko<sup>1,3</sup>, M. McGuire<sup>2,3</sup>, G. J. Evans<sup>2,3</sup>, and J. P. D.**  
6 **Abbatt<sup>1,3</sup>**

7 [1]{Department of Chemistry, University of Toronto, Toronto, Canada}

8 [2]{Department of Chemical Engineering and Applied Chemistry, University of Toronto,  
9 Toronto, Canada}

10 [3]{Southern Ontario Centre for Atmospheric Aerosol Research, University of Toronto,  
11 Toronto, Canada}

12 Correspondence to: J. P. D. Abbatt ([jabbatt@chem.utoronto.ca](mailto:jabbatt@chem.utoronto.ca))

1 **SI-1:** Unified dataset: Comparison of solutions at  $C_{PTR} = 5, 10,$  and 20

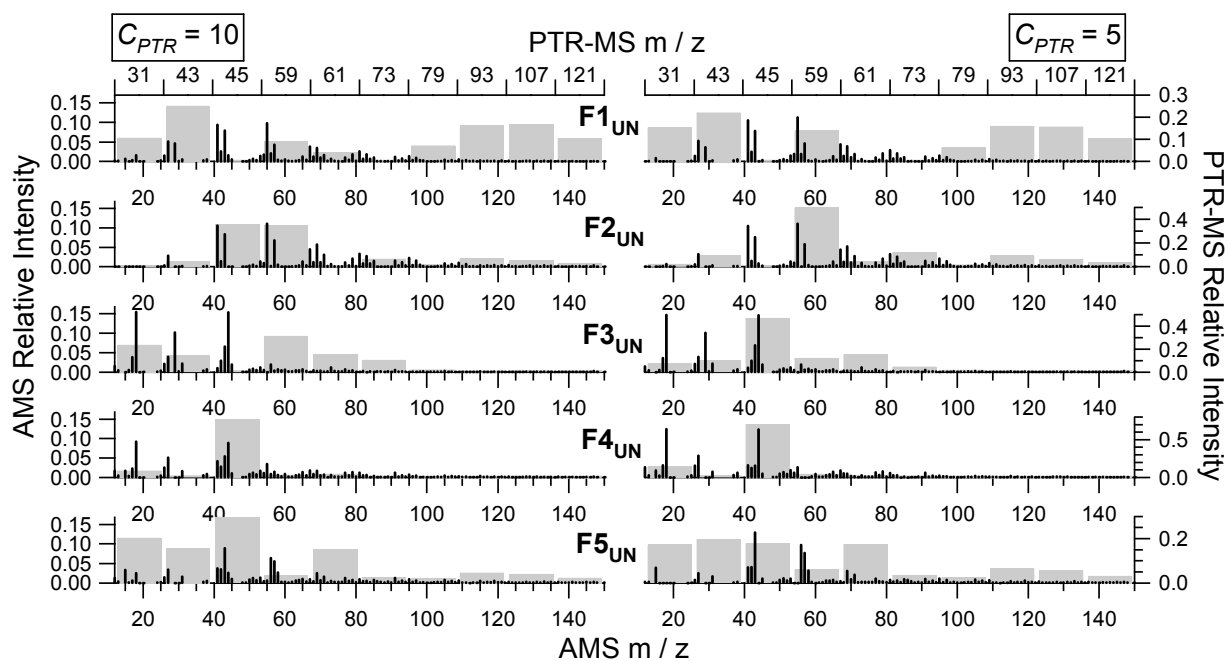
2  
3 As discussed in the main manuscript, the 5-factor solution at  $C_{PTR} = 10$  was  
4 selected as optimal. To further explore the solution space in terms of instrument  
5 weighting, we compare this selected solution to the 5-factor solutions obtained at  $C_{PTR} =$   
6 5 and  $C_{PTR} = 20$ , which are the adjacent points in Fig. 8. The mass spectra and time  
7 series of the  $C_{PTR} = 10$  solution are compared to that at  $C_{PTR} = 5$  in Figs. S5 and S6,  
8 respectively, and to  $C_{PTR} = 20$  in Figs. S7 and S8. In Fig. S9, we plot the fraction of  
9 signal apportioned to each factor for the AMS and at each PTR-MS  $m/z$ . The difference  
10 between the stacked  $m/z$ 's and 1 is due to signal contained in the residuals. The solutions  
11 are mostly similar, however the major differences are discussed below.

12 The most prominent change in the time series shown in Figs. S6 and S8 occurs in  
13 factor F3<sub>UN</sub>. As shown in Fig. S9, the AMS signal apportioned to F3<sub>UN</sub> decreases by  
14 approximately a factor of 3 between  $C_{PTR} = 10$  and  $C_{PTR} = 20$ . From Fig. S8, it is evident  
15 that the signal decreases both during the two discrete events on 30 January and during the  
16 extended 31 January to 2 February period. Proportionally, the 30 January event is  
17 decreased less than the extended period. As shown in Fig. S9, the decrease in the AMS  
18 fraction at F3<sub>UN</sub> corresponds with an increase in F1<sub>UN</sub>, which is mostly due to increased  
19 signal during the 31 January to 2 February period. The AMS F1<sub>UN</sub> mass spectrum is also  
20 affected, with the oxygenated marker  $m/z$  44 increasing from 1.6% of the spectrum at  
21  $C_{PTR} = 10$  to 4.1% at  $C_{PTR} = 20$ . Although this specific change is unique to the  $C_{PTR} = 20$   
22 solutions, it is representative of a general trend of increased similarity in AMS factor  
23 mass spectra with increasing  $C_{PTR}$ .

24 Changes in the PTR-MS factors are mostly due to reapportionment of acetone  
25 ( $m/z$  59) and acetic acid ( $m/z$  61) among the factors. Acetone and acetic acid  
26 apportionment is consistent between  $C_{PTR} = 10$  and  $C_{PTR} = 5$ . In contrast, at  $C_{PTR} = 20$ ,  
27 there is proportionally more acetone apportioned to F2<sub>UN</sub> and more acetic acid to F3<sub>UN</sub>.  
28 This is consistent with the emergence of factors dominated by acetone and acetic acid  
29 (i.e. factors F3<sub>PTR</sub> and F2<sub>PTR</sub>) as the PTR-MS weighting increases. A corresponding  
30 change in the AMS mass spectra of F2<sub>UN</sub> is observed, moving from hydrocarbon-like

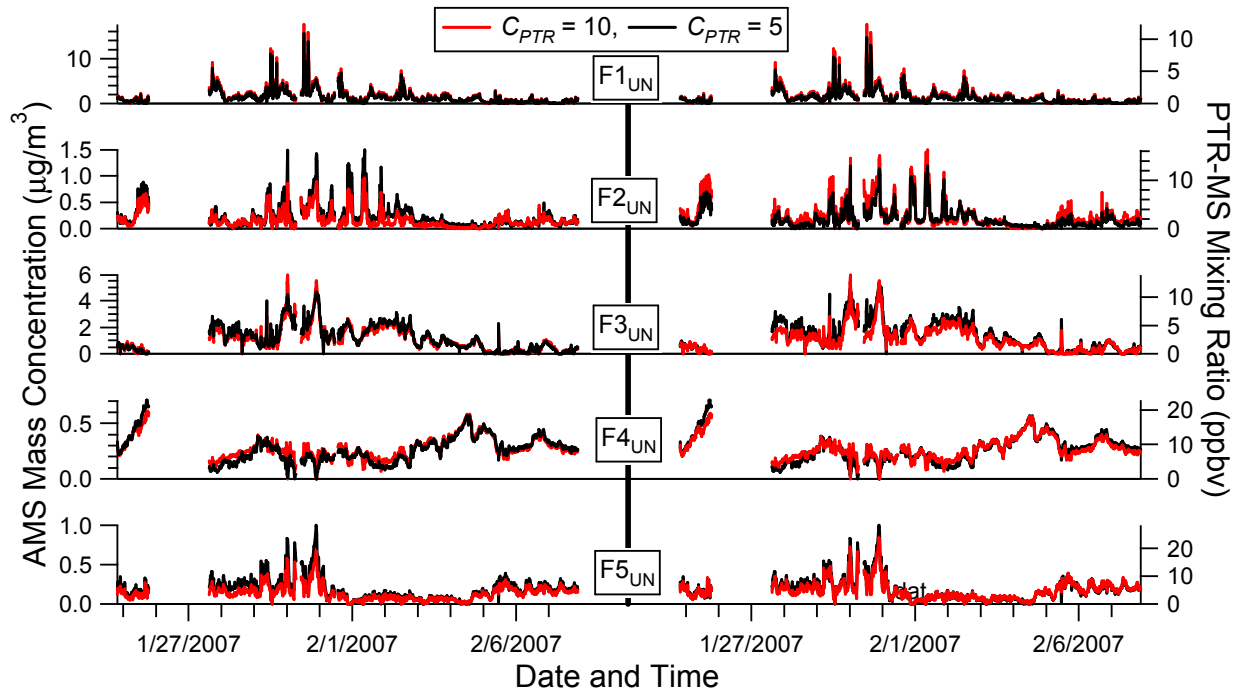
1 ( $C_{PTR} = 5$  and  $10$ ) to oxygenated ( $C_{PTR} = 20$ ). The oxygenated AMS spectrum is not  
2 consistent with the time series, which correlates with primary emission tracers such as  
3  $\text{NO}_x$  (see Fig. 11). This lack of self-consistency suggests that the AMS data is  
4 underweighted and therefore not reliable at  $C_{PTR} = 20$ . Because of this, the AMS data  
5 does not carry sufficient weight to enable the apportionment of acetone and acetic acid  
6 into primary and secondary sources, as was discussed in detail in the main manuscript.

7



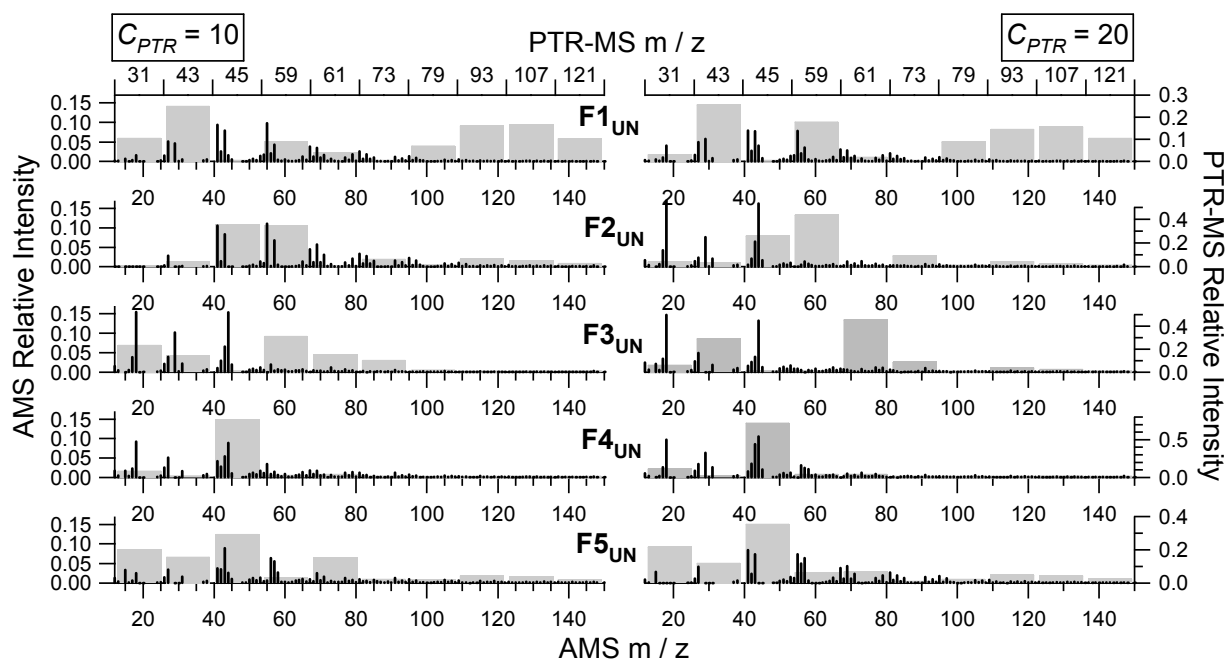
1

2 Figure S1. Factor mass spectra for the solutions to the unified dataset at  $C_{PTR} = 10$  (left  
 3 column) and  $C_{PTR} = 5$  (right column). AMS mass spectra are shown as black traces (left  
 4 and bottom axes); PTR-MS mass spectra are shown as grey bars (right and top axes).



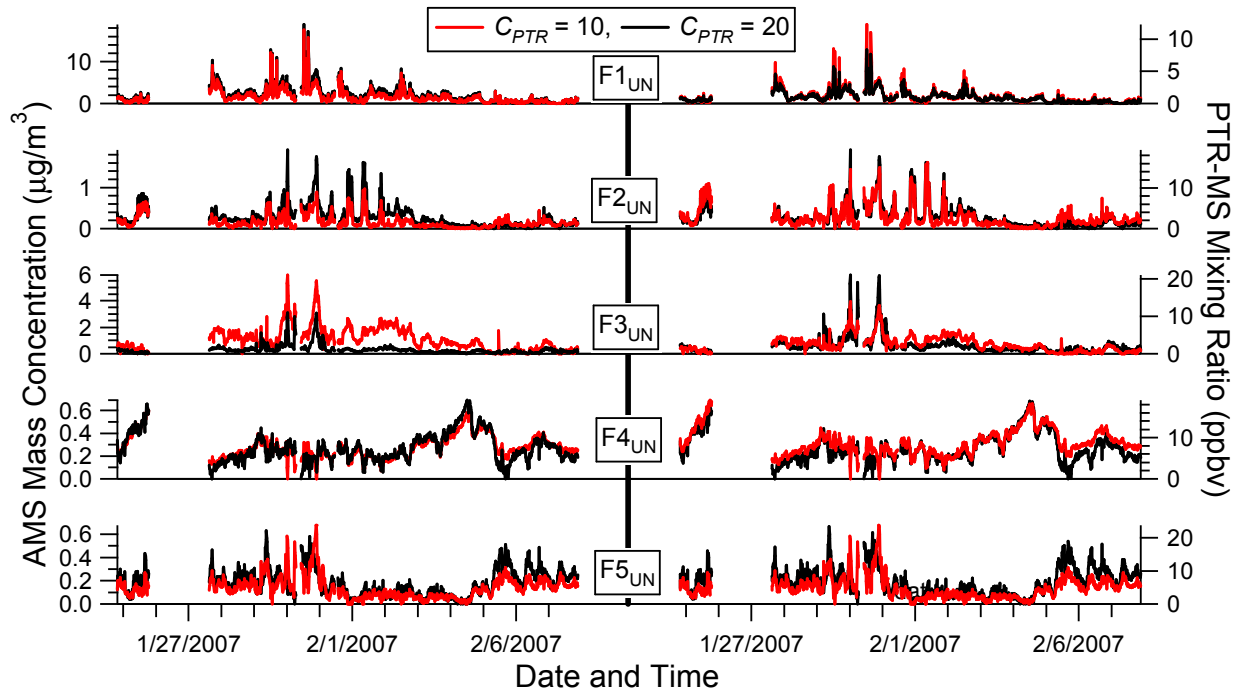
1

2 Figure S2. Factor time series for the solutions to the unified dataset at  $C_{PTR} = 5$  (black)  
 3 and  $C_{PTR} = 10$  (red). AMS and PTR-MS time series are shown on the left and right axes,  
 4 respectively.



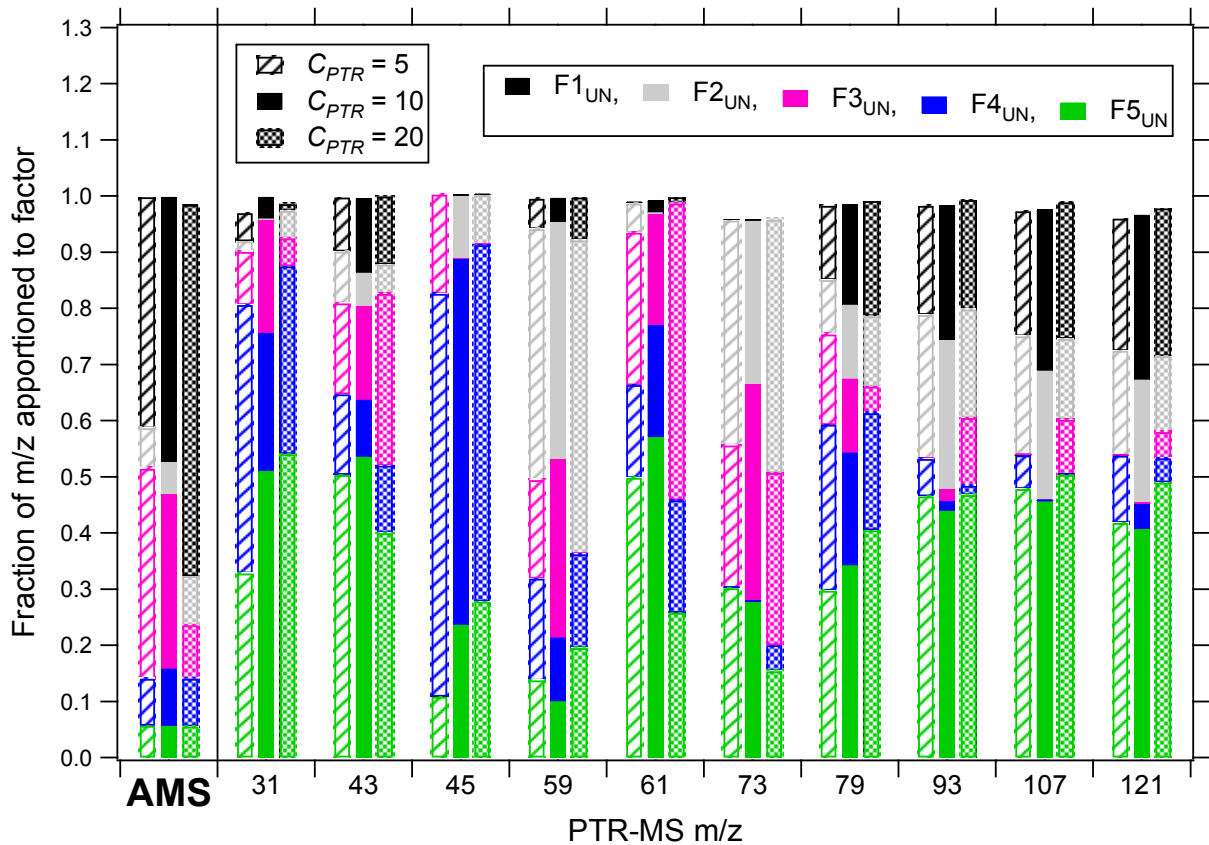
1

2 Figure S3. Factor mass spectra for the solutions to the unified dataset at  $C_{PTR} = 10$  (left  
 3 column) and  $C_{PTR} = 20$  (right column). AMS mass spectra are shown as black traces (left  
 4 and bottom axes); PTR-MS mass spectra are shown as grey bars (right and top axes).



1

2 Figure S4. Factor time series for the unified dataset solutions at  $C_{PTR} = 20$  (black)  
 3  $C_{PTR} = 10$  (red). AMS and PTR-MS time series are shown on the left and right axes,  
 4 respectively.



1

2 Figure S5. Mass spectra for the unified dataset solutions at  $C_{PTR} = 5, 10,$  and  $20$   
 3 represented as the fraction of signal in the AMS and at each PTR-MS  $m/z$  assigned to the  
 4 specified factor. Differences between the stacked total and 1 are due to signal contained  
 5 in the residuals.

6

7